Reviews

Surface Tension and Density of Liquid Metallic Alloys Measured by Electromagnetic Levitation†

Iván Egry* and Jürgen Brillo

Institut für Materialphysik im Weltraum, German Aerospace Center, DLR, 51170 Cologne, Germany

Reliable thermophysical data form the basis of any accurate solidification simulation. For the liquid phase of high-temperature metallic alloys, such data are scarce. In recent years, containerless methods, in particular electromagnetic levitation, have paved the way for noncontact measurement methods allowing precise determination of crucial thermophysical properties such as density, thermal expansion, and surface tension for this class of materials. Systematic investigations of the thermophysical properties of copper-based, nickel-based, and aluminum-based alloys have been carried out by the authors. This paper reviews the noncontact methodology used and provides a listing of the results obtained so far. Densities are discussed in terms of molar and excess volumes, whereas surface segregation is the key to understanding surface tensions of alloys.

Introduction

The precise knowledge of thermophysical properties becomes increasingly important as progress is made in numerical simulations of complex processes,[1] such as casting, welding, and surface treatment. Of particular importance are heat and mass flow in the liquid phase which significantly depend on thermophysical properties like surface tension and density. This can be most easily seen by considering the two dimensionless numbers characterizing buoyancy and surface tension driven convection, namely, the Rayleigh number Ra

$$Ra = \frac{L^4 \nabla T g \rho \beta}{\kappa \eta} \tag{1}$$

and the Marangoni number Ma

$$Ma = \frac{L^2 D\gamma}{\kappa \eta} \tag{2}$$

In these definitions, L is a characteristic length, ∇T a temperature gradient, g the gravitational acceleration, ρ the density, $\beta = -\rho^{-1}\partial\rho/\partial T$ the thermal expansion, κ the thermal diffusivity, η the viscosity, and, finally, $D\gamma$ the total differential of γ, given by

$$D\gamma = \frac{\partial \gamma}{\partial T}\nabla T + \frac{\partial \gamma}{\partial c}\nabla c \tag{3}$$

where the second term takes into account a concentration dependence of the surface tension of an alloy. As can be seen, convection is dominated by the derivatives of density and surface tension. While the temperature derivatives of these quantities can be considered constant over a wide temperature range, this is not the case for their concentration dependence.

With the improvement of the algorithms, the quality of a numerical simulation is limited by the accuracy of the input parameters characterizing the material under study. This is clearly shown in a quantitative way by recent sensitivity analyses.[2,3] Reliable data exist for low temperature liquids, but the situation is different for high temperature melts, like liquid metals with a melting temperature above 1300 K, typically. At these high temperatures, it is difficult to find a container that does not contaminate the specimen under investigation. The most comprehensive collection of data, apart from commercial databases, can still be found in the "Handbook of Physicochemical Properties at High Temperatures", published by the Iron and Steel Institute of Japan.[4]

For liquid metals, electromagnetic levitation provides containerless processing capabilities. An inhomogeneous rf electromagnetic field B exerts a Lorentz force $F \propto \nabla B^2$ on a metallic sample and lifts it against gravity. The ohmic power losses $P \propto B^2$ of the induced eddy currents in the sample heat and eventually melt the sample. In combination with noncontact diagnostic tools, this method is best suited for the study of liquid metals. Containerless processing has the additional advantage that liquid metals can be easily undercooled: due to the absence of container walls, the number of heterogeneous nucleation sites is greatly reduced, and nucleation is delayed. There is, however, one shortcoming of electromagnetic levitation: the electromagnetic fields not only lift and heat the sample but also deform its shape and induce potentially turbulent flows in the sample. These undesired side effects cannot be eliminated on Earth. For this reason, experiments under microgravity conditions are useful and have been performed.[5,6]

It is the main objective of this paper to provide a guide to recently obtained sets of highly reliable data measured by noncontact methods for a number of technically relevant binary and ternary metallic alloys. This paper focuses on two crucial thermophysical properties, namely, surface tension and density. For the latter, the discussion is based on the concept of molar excess volume,[7] while the Butler equation[8] provides the basis for understanding surface tensions of alloys. As most of the original data have been published previously, we restrict ourselves to representative examples and a synopsis of the available literature.

* Corresponding author. E-mail: ivan.egry@dlr.de.
† Part of the "William A. Wakeham Festschrift".

10.1021/je900119n CCC: $40.75
Published on Web 04/27/2009

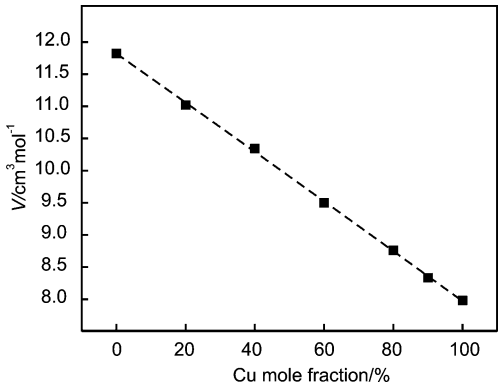

Figure 1. Molar volume, V, of liquid Ag−Cu at $T = 1270$ K (symbols), obeying eq 5 with $V^E = 0$ (dashed line) versus copper concentration.

Density

Densities of levitated samples are commonly measured using videography. In terrestrial levitation, samples are not spherical but slightly elongated due to the action of gravity and the electromagnetic field. However, their static equilibrium shape is still rotationally symmetrical around the vertical axis (parallel to the gravity vector). Therefore, images are taken perpendicular to this axis, and the volume V of a rotationally symmetrical body is calculated. The mass m of the sample is known; it is weighed before and after the measurement. The density of the sample is then obtained from

$$\rho = m/V \tag{4}$$

To maintain a temperature-independent contrast, the sample is illuminated from behind by monochromatic parallel laser light, and shadowgraphs are taken instead of direct images of the incandescent sample. In a first step, the software detects the edge of the sample for approximately 1000 snapshot images and calculates their average to remove potentially asymmetrical dynamic surface oscillations. In a second step, the shape of the average curve is fitted with a series of Legendre polynomials, and the volume is obtained from integration. This procedure leads to an error in density of less than 1 %.

For the thermal expansion, $\beta = -(\partial\rho/\partial T)\rho^{-1}$, the accuracy is less and can be estimated as (5 to 10) %. A detailed discussion has been given in ref 9.

The behavior of the density of alloys is best discussed in terms of the (molar) volume, because this is an extensive quantity in the thermodynamic sense. The molar volume of a binary alloy with elements A and B can be written as

$$V(c_A, c_B) = c_A V_A + c_B V_B + V^E(c_A, c_B) \tag{5}$$

where c_A and c_B are the concentrations; V_A and V_B are the molar volumes of the two alloy elements; respectively, and V^E is the so-called excess volume. Most conveniently, it can be expanded into Redlich−Kister polynomials.[10] To the lowest order in c_A and c_B, V^E can be written as $V^E(c_A, c_B) = c_A c_B V^x$, where V^x is a constant. In the case of a vanishing excess volume, eq 5 reduces to a simple linear combination of molar volumes V_i, which is often referred to as Vegard's law.[11]

An example for this case is the binary alloy system Ag−Cu whose molar volume is shown in Figure 1 for $T = 1270$ K as a function of the copper concentration. The data points collapse on the straight dashed line corresponding to eq 5 with $V^E = 0$. Hence, the molar volumes and the densities can be interpolated from the pure elements in this specific case.

For the vast majority of alloys, however, an excess volume which is either positive or negative has to be taken into account. This is demonstrated in Figure 2a and 2b for the binary alloys Al−Cu and Cu−Fe. In both figures, the experimental data points deviate from the linear (ideal) law with zero excess volume. In Figure 2a, this deviation is toward smaller values which corresponds to a negative excess volume, $V^E < 0$. In Figure 2b, it is the other way around. Both examples demonstrate the validity of eq 5 with the constant V^x being used as a fit parameter. The fit is shown by the solid lines in both diagrams which agree well with the experimental data.

It has been argued that the excess volumes are correlated with the enthalpies of mixing, which is physically plausible; it was shown, however, that this is not the case.[9]

Although a negative excess volume in amorphous binary alloys can be obtained using a bimodal distribution of solid spheres in model experiments,[12,13] the absolute value thus obtained is too low compared to experimental data on liquid metallic alloys, indicating that the observed excess volume cannot be explained based on geometrical arguments alone. Furthermore, a positive excess volume is only found in numerical simulations if more realistic interaction potentials of Lennard-Jones type with an attractive long-range part are used.[14]

During the past few years, we have measured the densities of a number of pure elements and binary alloys. Our data for the pure elements are shown in Table 1 in the form $\rho(T) = \rho_L - \rho'(T - T_L)$, where T_L is the liquidus temperature. All metals show a positive thermal expansion in the liquid phase, $\partial\rho/\partial T < 0$. The references to density data of binary alloys are shown in the lower left part of Table 2. In addition to pure elements and binaries, we have also studied the ternary systems Cu−Fe−Ni,

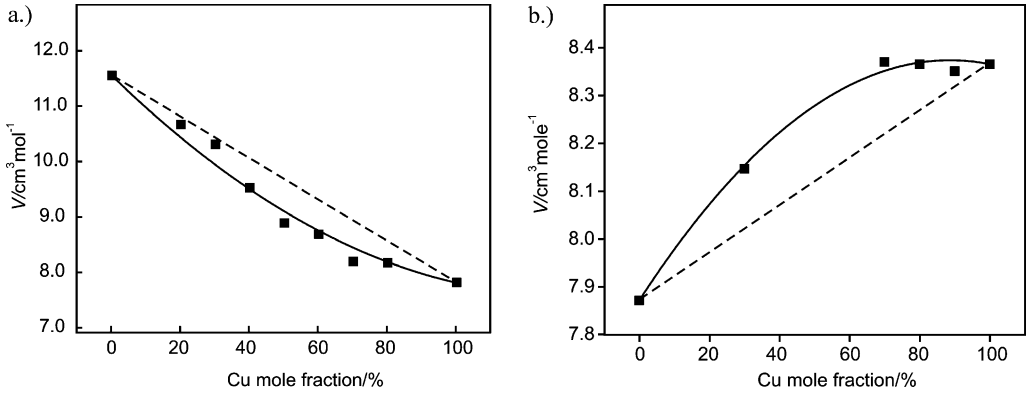

Figure 2. (a) Molar volume of Al−Cu at $T = 1020$ K (symbols) versus copper concentration obeying eq 5 with $V^E < 0$ (solid line). (b) Molar volume of Fe−Cu at 1760 K (symbols) versus copper concentration, obeying eq 5 with $V^E > 0$ (solid line). For comparison, both plots show eq 5 with $V^E = 0$ (dashed lines).

Table 1. Density and Surface Tension Data for Pure Liquid Metals, Measured by Electromagnetic Levitation at DLR

	T_L	ρ_L	ρ'		γ	γ'	
element	K	g·cm^{-3}	10^{-4} g·cm^{-3}·K^{-1}	ref	Nm^{-1}	10^{-4} N·m^{-1}·K^{-1}	ref
Ag	1235	9.15	7.4	15	0.91	1.8	16
Al	933	2.35	2.0	15	0.88	2.0	17
Au	1337	17.4	11	18	1.12	0.9	16
Co	1773	7.81	8.85	19	1.89	3.3	20
Cu	1357	7.90	7.65	9	1.29	2.34	21
Fe	1811	7.04	10.8	9	1.92	3.97	21
Ni	1727	7.92	10.1	9	1.77	3.3	21
Si	1683	2.52	3.53	22	0.784	6.5	23

Table 2. Thermophysical Data for Pure Elements and Binary Alloys, Measured at DLR[a]

	Al	Si	Cu	Ag	Au	Fe	Co	Ni
Al			27			28		28
Si			29					
Cu	15	29				21	20	21
Ag	15		18					
Au			30	18				
Fe	31		9				20	21
Co			19			19		
Ni	31		9			9		

[a] Upper right: references to surface tension data. Lower left: references to density data.

Table 3. References to Density and Surface Tension Data for Liquid Ternary and Multicomponent Alloys, Measured by DLR

alloy	density	surface tension
Cu−Fe−Ni	41	41
Cu−Fe−Co	19	19
Cu−Co−Ni	42	42
Al−Cu−Ag	43	44
Ti−6 atom % Al−4 atom % V		45
Ti−44 atom % Al−8 atom % Nb	46	46
CMSX-4		47

Cu−Fe−Co, Cu−Co−Ni, and Al−Cu−Ag extensively. Furthermore, a number of specific technical alloys have been investigated. References to these data are given in Table 3. On the basis of our data, we found the following general trends for the density:

• Alloys consisting of elements with a similar electronic configuration have no excess volume. Such alloys are Ni−Fe, Co−Fe, Cu−Ag, Cu−Au, and Au−Ag.

• Copper-based alloys containing a transition metal showed a positive excess volume. Alloys for which we found such a behavior are: Cu−Fe, Cu−Co, Cu−Fe−Ni, and Cu−Co−Fe. These alloys also exhibit a metastable liquid miscibility gap. The only exception in this class may be Cu−Ni and Cu−Ni−Co for which $V^E < 0$ was found.[9]

• Al-based alloys, such as Al−Fe, Al−Ni, Al−Cu, and Al−Cu−Ag, show a strongly negative excess volume. These alloys are usually characterized by an exothermic mixing behavior, and their phase diagrams exhibit intermetallic phases.

Surface Tension

The oscillating drop technique is an elegant way to measure the surface tension γ. It employs digital image processing for frequency analysis of surface oscillations. The surface of a liquid droplet undergoes oscillations sustained by its surface tension. The frequencies of the oscillations are therefore related to the surface tension. If the equilibrium shape of the droplet is spherical, the lowest observable frequency is the Rayleigh frequency ω_R given by

$$\omega_R^2 = \frac{32\pi}{3}\frac{\gamma}{m} \tag{6}$$

where m is the mass of the droplet. A spherical shape is obtained only if the droplet is free of external forces. This situation is well approximated in microgravity. Under terrestrial conditions, the above relation is not valid: the external fields lead to a splitting of the single frequency into five shifted frequencies $\omega_{2,m}$. These effects can be taken into account by using the following correction formula derived by Cummings and Blackburn[24]

$$\frac{32\pi}{3}\frac{\gamma}{m} = \frac{1}{5}\sum_m \omega_{2,m}^2 - 1.9\overline{\Omega_{tr}^2} - 0.3(\overline{\Omega_{tr}^2})^{-1}(g/a)^2 \tag{7}$$

Here, $\overline{\Omega_{tr}^2}$ is the mean of the squared translational frequencies of the sample in the potential of the levitation field; a is the radius of the drop; and g is the gravitational acceleration. It has been shown that by applying this correction to surface tension data obtained by the oscillating drop technique on Earth a spurious mass dependence can be eliminated.[25] Egry and coworkers have performed microgravity experiments on a gold−copper alloy.[26] These experiments clearly show a single peak in the oscillation spectrum, and furthermore, they yield values for the surface tension which are in excellent agreement with terrestrial data only if the latter are corrected according to eq 7. After such correction, the accuracy of surface tension data measured by the oscillating drop technique is better than 5 %. As in the case of thermal expansion, the error in the temperature coefficient $\partial\gamma/\partial T$ is larger and is about 20 %. As $\partial\gamma/\partial T = -s_\gamma$, where s_γ is the surface entropy, it is always negative for pure elements.

The major experimental difficulty in surface tension measurements at high temperatures lies in the control of the processing atmosphere and the purity of the sample material. Oxygen and sulfur are both surface active in liquid metals. Already, a few parts per million of soluble oxygen can lead to a reduction of the surface tension by more than 10 %[32] and even to a reversal of the sign of $\partial\gamma/\partial T$. The influence of oxygen on the surface tension has been studied by Mukai[33] for Si and, more generally, by Hibiya.[34] It is most conveniently described by Belton's equation

$$\gamma = \gamma_0 - RT\ln(1 + K_0 p_{O_2}^{1/2}) \tag{8}$$

where γ_0 is the surface tension in the absence of oxygen; R is the universal gas constant; p_{O_2} is the oxygen partial pressure; and K_0 is the adsorption coefficient, which is related to excess thermodynamic enthalpy ΔH and entropy ΔS by

$$K_0 = \exp\left(-\frac{\Delta H - T\Delta S}{RT}\right) \tag{9}$$

Oxygen may come from the processing atmosphere (even 6N purity bottles of inert gases contain oxygen), leaks of the process chamber and gas lines, a substrate, or the sample itself. In containerless processing, contamination from a substrate can be excluded, and the samples can be purified in situ by overheating the melt to a temperature where volatile oxides form which can be pumped out. Contamination due to process gas and leakage could only be avoided by processing under ultrahigh vacuum. In most cases, however, the high evaporation rates of

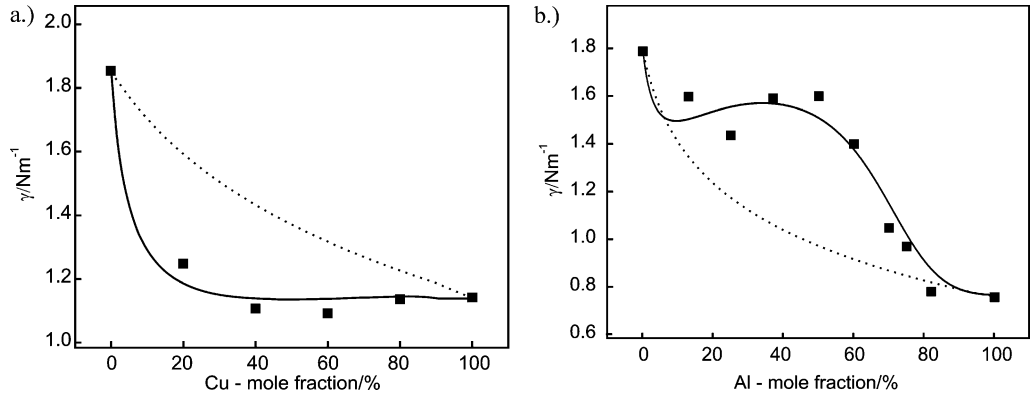

Figure 3. (a) Surface tension of Cu−Fe at 1970 K versus copper mole fraction (symbols) showing a steep decrease at small concentrations. Shown is also a plot of the solution of the Butler equation (solid line) and of the ideal solution model (dashed line). (b) Surface tension of Ni−Al at 1670 K versus aluminum concentration (symbols) with the appearance of a shoulder. The solid line corresponds to a simple model for the effect of associate formation, the dashed line to the ideal solution model.

liquid metals prohibit such an approach. Nevertheless, it is fair to say that containerless processing is less prone to oxygen contamination than container-based methods.

According to Gibbs, the surface can be treated as a separate thermodynamic phase which is in thermal equilibrium with the bulk. As a consequence, the surface tension of an alloy can be calculated from thermodynamic principles. The most common model used is due to Butler,[8] who treated the surface as a monolayer, with surface thermodynamic potentials of the same functional form as the bulk phases, but reduced in strength by the percentage of missing atomic bonds at the surface. For binary alloys, Butler's equation reads

$$\begin{aligned}\gamma_{AB}(T) &= \gamma_A + \frac{RT}{A_A}\ln\left(\frac{1 - c^S_B}{1 - c^B_B}\right) + \\ &\quad \frac{1}{A_A}\{\Delta G^S_A(T, c^S_B) - \Delta G^B_A(T, c^B_B)\} \\ &= \gamma_B + \frac{RT}{A_B}\ln\left(\frac{c^S_B}{c^B_B}\right) + \\ &\quad \frac{1}{A_B}\{\Delta G^S_B(T, c^S_B) - \Delta G^B_B(T, c^B_B)\}\end{aligned} \tag{10}$$

Here, γ_A and γ_B are the surface tensions of the pure elements; T is the temperature; R is the universal gas constant; A_A and A_B are the surface areas occupied by atoms of species A and B; c^S_B is the concentration of species B at the surface; $\Delta G^B_{A,B}$ are the partial Gibbs excess free energies of species A or B, respectively, in the bulk; and $\Delta G^S_{A,B}$ is the same quantity for the surface. According to Tanaka,[35] ΔG^S can be put to $\Delta G^S = 0.75\Delta G^B$ for liquid metals. Finally, the specific surface areas can be calculated from the molar volumes according to $A_X = 1.091(N_A)^{1/3}V_X^{2/3}$ (X = A,B), where N_A is Avogadro's constant. Equation 10 is an equation for the unknown surface concentration c^S_B. Once it is solved, γ_{AB} follows directly. The extension of the Butler approach to multicomponent alloys is possible, but cumbersome. For such systems, a different formulation, based on the original Gibbsian approach, has been suggested and applied to the ternary system Ag−Au−Cu.[36]

For the case of vanishing excess Gibbs energies, eq 10 can be solved analytically. This yields the ideal solution model, which takes into account the entropy of mixing only. In the ideal solution model, the surface tension γ_{AB} is given by

$$\gamma_{AB} = \frac{\gamma_A c_A}{c_A + c_B/S_0} + \frac{\gamma_B c_B}{c_B + c_A S_0} \tag{11}$$

with the segregation factor S_0 given by[37]

$$S_0 = e^{A(\gamma_B - \gamma_A)/RT} \tag{12}$$

Here $A = A_A = A_B$ is the specific surface area as before, assumed to be the same for both species. Although quantitatively incorrect, the ideal solution model describes the most prominent feature of liquid alloys qualitatively correctly: surface segregation. In an alloy, the component with the lowest surface tension tends to segregate at the surface to reduce the system's total energy. The segregation profile is determined by the interplay between energetic and entropic effects. Surface segregation leads to a concave shape of the surface tension as a function of concentration, i.e., a lowering of the surface tension below the linear interpolation between the two constituent elements. This is shown in Figure 3a for Cu−Fe as an example. The excess free enthalpy is positive for this alloy, and the surface tension is generally lower than expected for the ideal solution. As predicted from the Butler equation, pronounced segregation of copper takes place at the surface layer. The surface mole fraction of copper is larger than 80 % already for small copper bulk mole fraction of $c^B_{Cu} > 15$ %.

The Al−Ni system, displayed in Figure 3b, represents an alloy which is characerized by the presence of intermetallic solid phases in the phase diagram and excess free enthalpies $\Delta G^B_{A,B} \ll 0$. As visible in Figure 3b, the surface tension plot has a convex shape and lies above the ideal solution curve and the linear interpolation. The remarkable feature in this plot is a broad maximum around an Al mole fraction of 50 % following a dip at approximately 25 %. This behavior can be explained by the presence of associates or clusters in the melt which prevent segregation of the otherwise surface-active species at the surface. A quantitative description of such behavior is possible in the framework of the compound formation model.[38] A simple model,[37] based on an extension of the segregation factor S_0, is capable of fitting the data correctly. This is also shown in Figure 3b.

Generally speaking, one may state that alloys with a demixing tendency, i.e., with interactions favoring homoatomic pairs, tend to show stronger segregation and a negative deviation from ideal solution, while the opposite is true for systems which prefer

heteroatomic pairs, in particular those displaying stable solid intermetallic compounds.

The temperature coefficient, $\partial\gamma/\partial T$, can have both signs for an alloy since the surface concentrations differ from those in the bulk, giving rise to chemical ordering effects.

The surface tensions of the pure elements have been compiled by Keene[39] and recently updated by Mills.[40] Our own data are shown in Table 1 in the form $\gamma(T) = \gamma_L - \gamma'(T - T_L)$, where T_L is the liquidus temperature. Keene has also reviewed the surface tension of iron and its binary alloys.[32] Tanaka and Iida have calculated the surface tensions of iron-based alloys using Butler's equation and a thermodynamic database.[35] References to our surface tension measurements of binary alloys are given in the upper right diagonal of Table 2 and in the second column of Table 3 for multicomponent systems.

Summary and Outlook

Noncontact measurement methods will become the benchmark experiments for thermophysical properties of high-temperature metallic liquids, in particular, if and when these measurements will be carried out in a microgravity environment. These data can be used as temperature and concentration dependent input parameters for complex simulation tools. To understand multicomponent technical alloys, it is first necessary to study the basic phenomena, like excess volume and surface segregation, systematically in the underlying binary system.

Acknowledgment

The authors want to acknowledge many fruitful discussions with W. Wakeham about the measurements of thermophysical properties in general and, in particular, about the utilization of microgravity platforms for such purpose. Fruitful discussions with all project partners are gratefully acknowledged.

Literature Cited

(1) Hepp, E.; Neves, S.; Egry, I. High precision measurements of thermophysical properties of liquid metals − Requirements for simulation of foundry processes with MAGMASOFT. *Modeling of Casting, Welding and Advanced Solidification Processes IX*; Sahm, P., Hansen, P., Conley, J., Eds.; Shaker Verlag Aachen, 2000; pp 697−703.

(2) Drezet, J.; Commet, B.; Fjaer, H.; Magnin, B. Stress-strain computations of the DC casting process of aluminium alloy: a sensitivity study on material properties. *Modeling of Casting, Welding and Advanced Solidification Processes IX*; Sahm, P., Hansen, P., Conley, J., Eds.; Shaker Verlag Aachen, 2000; pp 33−40.

(3) Ebrahimi, S.; Tortorelli, D.; Dantzig, J. Sensitivity analysis and nonlinear programming applied to investment casting design. *Appl. Math. Modell.* **1997**, *21*, 113–123.

(4) Kawai, Y., Sharaishi, Y., Eds. *Handbook of Physico-chemical Properties at High Temperatures*; The Iron and Steel Institute of Japan, 1988.

(5) Team TEMPUS. Containerless Processing in Space: Recent Results; *Materials and Fluids under low gravity*; Ratke, L., Walter, H., Feuerbacher, B., Eds.; Springer: Berlin, 1996; pp 233−252.

(6) Egry, I. Properties, Nucleation and Growth of Undercooled Liquid Metals: Results of the TEMPUS MSL-1 Mission. *J. Jpn. Soc. Microgravity Appl.* **1998**, *15*, 215–224.

(7) Iida, T.; Guthrie, R. *The Physical Properties of Liquid Metals*; Clarendon Press: Oxford, 1993.

(8) Butler, J. The thermodynamics of the surfaces of solutions. *Proc. R. Soc. A* **1932**, *135*, 348–375.

(9) Brillo, J.; Egry, I. Density and excess volumes of Cu, Ni, Fe, and their alloys. *Z. Metallkd.* **2004**, *95*, 691–697.

(10) Hillert, M. Thermodynamic Modelling of Solutions. *CALPHAD* **1997**, *21*, 143–154.

(11) Vegard, L. Die Konstitution der Mischkristalle und die Raumfüllung der Atome. *Z. Phys.* **1921**, *5*, 17–26.

(12) Lemaignan, C. Hard Spheres simulation of the size effect in liquid and amourphous metallic alloys. *Acta Metall.* **1980**, *28*, 1657–1661.

(13) Khantadze, D. V.; Topuridze, N. I. *Compression Mechanism for Two-Component Loose Media Modeled By Spherical Particles*; Institute of Metallurgy, Academy of Sciences of the Georgian SSR: Tilisi, Translated from Inzhenerno-Fizicheskii Zhurnal, 1977; Vol. 33, pp 120−125.

(14) Blas, F.; Fujihara, I. Excess properties of Lennard-Jones binary mixtures from computer simulation and theory. *Mol. Phys.* **2002**, *100*, 2823–2838.

(15) Brillo, J.; Egry, I.; Westphal, J. Density and thermal expansion of liquid binary Al-Ag and Al-Cu alloys. *Int. J. Mater. Res.* **2008**, *99*, 162–167.

(16) Egry, I.; Sauerland, S.; Jacobs, G. Surface Tension Measurements on Levitated Liquid Noble Metals. *High Temp.−High Press.* **1994**, *26*, 217–223.

(17) Egry, I.; Schneider, S.; Seyhan, I.; Volkmann, T. Surface Tension Measurements of High Temperature Metallic Melts. *Trans JWRI* **2001**, *30*, 195–200.

(18) Brillo, J.; Egry, I.; Ho, I. Density and Thermal Expansion of Liquid Ag-Cu and Ag-Au Alloys. *Int. J. Thermophys.* **2006**, *27*, 494–506.

(19) Brillo, J.; Matsushita, T.; Egry, I. Density and Thermal Expansion of liquid binary and ternary Cu-Co-Fe- alloys. *Int. J. Mater. Res.* **2006**, *97*, 1526–1531.

(20) Eichel, R.; Egry, I. Surface tension and surface segregation of liquid cobalt-iron and cobalt-copper alloys. *Z. Metallkd.* **1999**, *90*, 371–375.

(21) Brillo, J.; Egry, I. Surface tension of nickel, copper, iron and their binary alloys. *J. Mater. Sci.* **2005**, *40*, 2213–2216.

(22) Egry, I.; Jacobs, G.; Gorges, E.; Langen, M. Measurement of the density and the thermal expansion coefficient of molten silicon using electromagnetic levitation. *J. Cryst. Growth* **1998**, *186*, 550–556.

(23) Przyborowsky, M.; Hibiya, T.; Eguchi, M.; Egry, I. Surface Tension Measurement of molten silicon by the oscillating drop method using electromagnetic levitation. *J. Cryst. Growth* **1995**, *151*, 60–65.

(24) Cummings, D.; Blackburn, D. Oscillations of magnetically levitated aspherical droplets. *J. Fluid Mech.* **1991**, *224*, 395–416.

(25) Egry, I.; Sauerland, S. Containerless processing of undercooled melts: measurements of surface tension and viscosity. *Mater. Sci. Eng., A* **1994**, *178*, 73–76.

(26) Egry, I.; Lohöfer, G.; Jacobs, G. Surface Tension of Liquid Metals: Results from Measurements on Ground and in Space. *Phys. Rev. Lett.* **1995**, *75*, 4043–4046.

(27) Schmitz, J.; Brillo, J.; Egry, I., to be published.

(28) Egry, I.; Brillo, J.; Holland-Moritz, D.; Plevachuk, Y. The surface tension of liquid aluminium-based alloys. *Mater. Sci. Eng. A* **2008**, *495*, 14–18.

(29) Adachi, M.; Brillo, J.; Egry, I.; Watanabe, M., to be published.

(30) Brillo, J.; Giffard, H.; Patti, A.; Egry, I. Density and thermal expansion of levitated Cu-Au alloys. *Int. J. Thermophys.* **2003**, *25*, 1881–1888.

(31) Plevachuk, Y.; Egry, I.; Brillo, J.; Holland-Moritz, D.; Kaban, I. Density and atomic volume in liquid Al-Fe and Al-Ni binary alloys. *Int. J. Mater. Res.* **2007**, *98*, 107–111.

(32) Keene, B. Review of data for the surface tension of iron and its binary alloys. *Int. Mater. Rev.* **1988**, *33*, 1–37.

(33) Mukai, K.; Yuan, Z.; Nogi, K.; Hibiya, T. Effect of the Oxygen Partial Pressure on the Surface Tension of Molten Silicon and ist Temperature Coefficient. *ISIJ Int.* **2000**, *40 suppl.* , S148−S152.

(34) Morohoshi, K.; Hibiya, T., to be published.

(35) Tanaka, T.; Iida, T. Application of a thermodynamic database to the calculation of surface tension for iron-base liquid alloys. *Steel Res.* **1994**, *65*, 21–28.

(36) Pajarre, R.; Koukkari, P.; Tanaka, T.; Lee, J. Computing surface tensions of binary and ternary alloy systems with the Gibbsian method. *CALPHAD* **2006**, *30*, 196–200.

(37) Egry, I. The Surface Tension of Binary Alloys: Simple Models for Complex Phenomena. *Int. J. Thermophys.* **2005**, *26*, 931–939.

(38) Bhatia, A.; Hargrove, W. Concentration fluctuations and thermodynamic properties of some compound forming binary molten systems. *Phys. Rev. B* **1974**, *10*, 3186–3196.

(39) Keene, B. Review of data for the surface tension of pure metals. *Int. Mater. Rev.* **1993**, *38*, 157–192.

(40) Mills, K.; Su, Y. Review of Surface Tension Data for Metallic Elements and Alloys, Part I: Pure Metals. *Int. Mater. Rev.* **2006**, *51*, 329–351.

(41) Egry, I.; Brillo, J.; Matsushita, T. Thermophysical Properties of Liquid Cu-Fe-Ni Alloys. *Mater. Sci. Eng. A* **2005**, *413−414*, 460–464.

(42) Schick, M.; Brillo, J.; Egry, I. Thermophysical properties of liquid Co-Cu-Ni alloys. *Int. J. Cast Metals Res.*, to be published.

(43) Brillo, J.; Brooks, R.; Egry, I.; Quested, P. Density and viscosity of liquid ternary Al-Cu-Ag alloys. *High. Temp.−High. Press.* **2008**, *37*, 371–381.

(44) Brillo, J. Egry, I. Thermal Expansion and Surface Tension of Multicomponent Alloys. *Phase Transformations in Multicomponent Melts*; Herlach, D. M., Ed.; Wiley-VCH: Weinheim, 2008; pp 55−71.

(45) Schneider, S.; Egry, I.; Seyhan, I. Measurement of the Surface Tension of Undercooled Liquid $Ti_{90}Al_6V_4$ by the Oscillating Drop Technique. *Int. J. Thermophys.* **2002**, *23*, 1241–1248.

(46) Brillo, J.; Schneider, S.; Egry, I.; Harding, T. Density, Thermal Expansion and Surface Tension of Liquid Titanium Alloys Measured by Non-Contact Techniques. *Ti-2003 Science and Technology*; Lütjering, G., Albrecht, J., Eds.; Wiley-VCh: Weinheim, 2004; pp 411−417.

(47) Vinet, B.; Schneider, S.; Garandet, J. P.; Marie, B.; Drevet, B.; Egry, I. Surface tension measurements on CMSX-4 super-alloy by the drop-weight and oscillating drop methods". *Int. J. Thermophys.* **2004**, *25*, 1889–1903.

Received for review January 29, 2009. Accepted April 12, 2009. Parts of the work were performed under contracts with the European Space Agency, ESA, in the CoolCop and Thermolab projects. We also thank the German Science Foundation DFG for partial support of the work presented here.

JE900119N